Transient Effects in Arterial CBV Quantification

Kathrin Lorenz, Toralf Mildner, André Pampel, & Harald E. Möller

Max Planck Institute for Human Cognitive and Brain Sciences, Leipzig, Germany

klorenz@cbs.mpg.de

Introduction

Recently, the inflow-based vascular-space-occupancy (iVASO) approach [1] was extended to measure absolute values of arterial cerebral blood volume (aCBV) [2,3]. Briefly, the contrast is obtained by acquiring pairs of images: for the 'null condition' (N) with the inflowing blood nulled at the inversion time (*TI*) and for the 'control condition' (C) without blood nulling (Fig. 1). The difference images, C–N, are used to calculate aCBV.

Purpose of the current study was to investigate transient effects in aCBV quantification in case of long *TI*s which might be required either to fulfill the specific absorption rate (SAR) constraints at higher magnetic field strengths or to allow for an adequate filling of the vascular space with inverted blood magnetization (i.e. labeled arterial blood) in case of flow-weighted (FW) iVASO experiments [4]. The inflow dynamics of labeled arterial blood was investigated by varying the slice thickness and its ratio to the width of the slice-selective inversion pulse (Fig. 1) whereas the influence of 'fresh' (i.e. non-labeled) arterial blood was studied by varying the width of the non-selective inversion pulse. Application of mild FW gradients removes signal contributions of large arteries that perforate the imaging slice and therefore accounts for determination of blood that is distributed within the imaging slice.

1

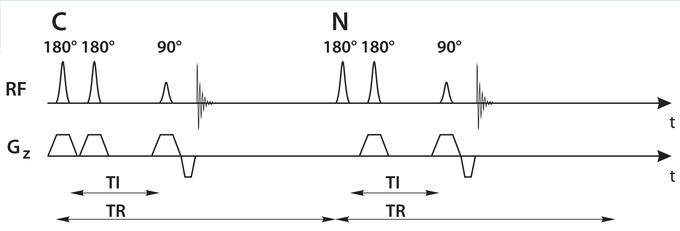

Pulse sequence scheme as employed for iVASO in this study and in Ref. [2].

Methods

- 3-T whole-body scanner (Bruker MedSpec 30/100) & birdcage coil.
- 10–12 ms sech inversion pulse & 1.5–2 ms 90° hermite excitation pulse.
- 5 *TI/TR* pairs fulfilling the blood nulling condition, cf. Ref. [2].
- Gradient-echo EPI, bandwidth 100 kHz, 50 C–N pairs per *TI/TR* pair.
- Bipolar FW gradients along z-axis; b-values of 0 and 2 s/mm^2.
- Axial slice, nominal resolution 3 x 3 x 2 mm^3 and 3 x 3 x 4 mm^3.
- Experimental and evaluation procedure as given in Ref. [4].

Results & Discussion

Figure 2 presents *TI* curves obtained from iVASO experiments in the territory of the middle cerebral artery (MCA) for individual subjects. In the top row, experiments with (red curves) and without FW gradients are shown whereas, in the bottom row, inversion gaps, i.e. minimum distances for the label to reach the imaging slice, of 1.8 mm (red curves) and 0.4 mm are compared in experiments with FW gradients. The overall inter-subject variability was lowest if mild FW gradients were applied, and a sufficiently large inversion gap is maintained. Then, the inflow dynamics showed an exponential behavior and was roughly independent of the slice thickness, cf. all red curves in Fig. 2. An example of the corresponding aCBV maps as function of *TI* is depicted in Fig. 3.

Both above findings can be explained by signal contributions from large arteries. Vessels that perforate the voxel of interest instead of perfusing it are highly variable in their location and/or orientation. The removal of this contribution by FW gradients therefore reduces the aCBV variability not only between regions but also between subjects. The increased inter-subject variability at the smaller inversion gap is likely due to a restoring of signals from feeding arteries that are aligned almost parallel to the imaging slice and for which the FW gradients act less efficient.

Figure 4 shows group averaged *TI* curves of aCBV from the FW experiments with a reasonable choice of the inversion gap for the territories of the MCA and the posterior cerebral artery (PCA) at nominal resolutions of 3 x 3 x 2 mm^3 and 3 x 3 x 4 mm^3. For parametrization, an exponential fit, cf. Table 1, was applied, yielding three parameters: the estimated aCBV value, $aCBV_\infty \approx 1.1–1.9$ %, the time constant of the exponential fit, $\tau \approx 100–200$ ms, and the starting time of the inflow, $TI_0 \approx 700–800$ ms. A general observation is that inflow in the PCA territory occurred delayed and more slowly as compared to the MCA territory. This might be due to a regionally varying cerebral perfusion pressure (CPP). $aCBV_\infty$ estimates were very similar across territories and slice thicknesses except for the PCA territory of the thicker slice.

Finally, the contamination of the aCBV values by 'fresh' arterial blood was investigated in experiments with different widths of the non-selective inversion pulse (Fig. 5). In case of the smaller inversion width, the transit time of 'fresh' arterial blood from beyond the inversion area is shortened artificially. The effect on the aCBV transients can be described on a qualitative level. At short *TI*, 'fresh' blood will be present in the C condition only, and the C–N signal difference will be artificially increased. If *TI* is long enough to obtain 'fresh' blood contamination also in the N condition, the C–N signal difference decreases. Hence, any decline of the aCBV transient can be interpreted as a 'fresh' blood contamination. Without FW, all transients shown in Fig. 5 show such a decline in case of the small inversion width. It is also evident that the 'fresh' blood contamination is stronger for the MCA than the PCA territory which is in agreement with the arterial blood transit time difference from the human neck between both territories [5]. With FW, a decline occurs only in case of the MCA territory for the small inversion width (Fig. 5) which clearly demonstrates that FW gradients are capable of reducing 'fresh' blood contaminations. However, the overestimation of aCBV due to 'fresh' blood at short *TI*s can still hardly be distinguished, and the observed faster inflow in the MCA (Fig. 4) at the maximum inversion width (as defined by the transmit profile of the RF coil) might in part be due to this effect.

To conclude, blood delivery by vessels of variable size cause transient effects in aCBV quantification. Application of mild FW gradients diminish these effects and provide a better inter-subject stability and a lower sensitivity to both 'fresh' blood effects and the influence of large arteries that perforate the voxels of interest.

2

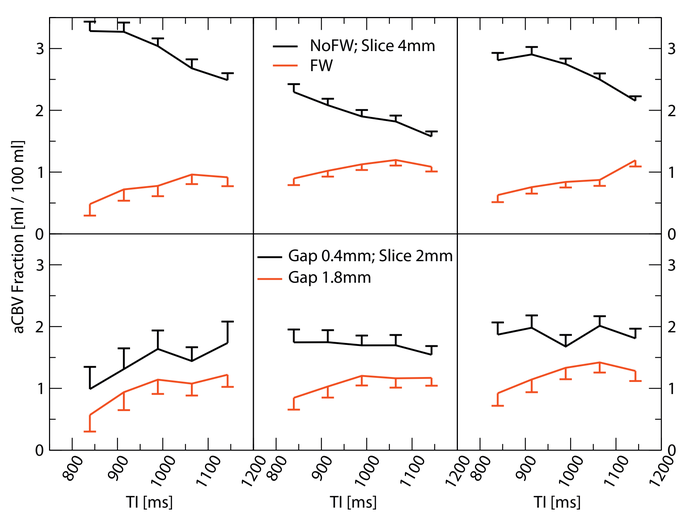

TI dependency of aCBV obtained in the MCA territory for individual subjects at nominal resolutions of 3x3x4 mm3 (top) comparing experiments with and without FW and of 3x3x2 mm3 (bottom) comparing experiments of variable inversion gaps.

4

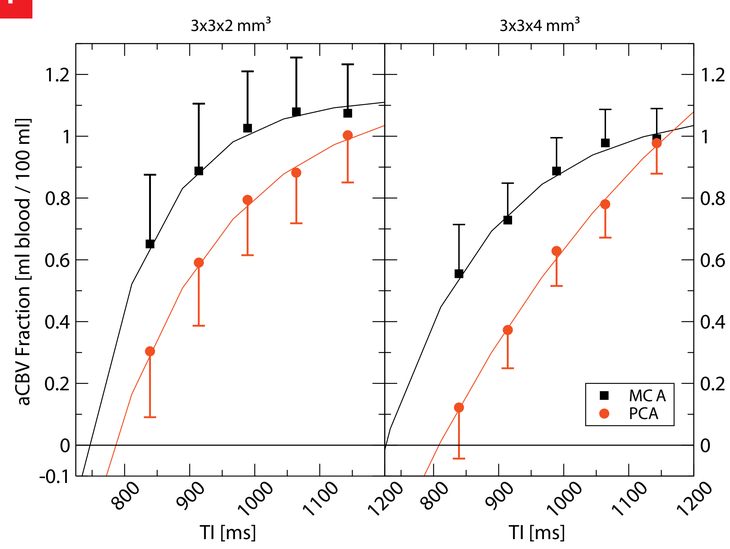

TI dependence of aCBV obtained by averaging over at least 6 individual subjects in the MCA (black squares) and PCA territory (red circles). The results were fitted by an exponential function, cf. Table 1, (solid lines).

5

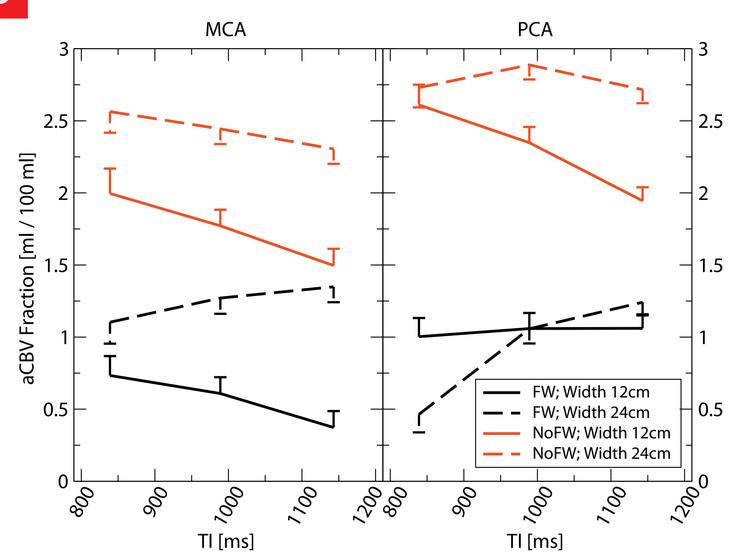

TI dependence of aCBV in the MCA and PCA territory obtained in a single subject. Results were obtained at inversion widths of 12 cm (solid) and 24 cm (dashed) without (red) and with (black) FW at a nominal resolution of 3x3x4 mm3.

3

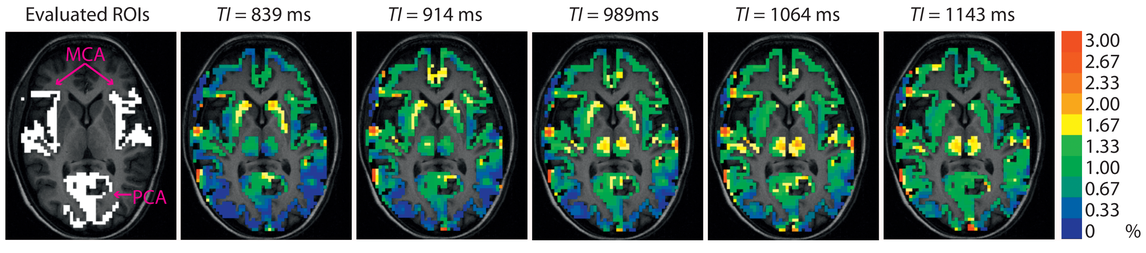

Maps of aCBV at 3 x 3 x 4 mm^3 resolution acquired in the same subject with FW for variable *TI*.

Table 1

Fit Parameters	MCA		PCA	
$aCBV(t) = aCBV_\infty - a*\exp(-t/\tau)$	3x3x2 mm^3	3x3x4 mm^3	3x3x2 mm^3	3x3x4 mm^3
$aCBV_\infty$ [%]	1.1	1.1	1.1	1.9
τ [ms]	109	164	182	482
TI_0 [ms]	747	727	787	808

Fit function that is applied to the group averages displayed in Fig. 4 and the resulting fit parameters.

References

[1] J. Hua et al.; *Magn Reson Med* 2011; 66: 40–56.
[2] M.J. Donahue et al.; *J Cereb Blood Flow Metab* 2010; 30:1329–1342.
[3] J. Hua et al.; *NMR Biomed* 2011; 24: 1313–1325.
[4] K. Lorenz et al.; *Proc. ISMRM* 19 2011; 3854.
[5] T. Mildner et al.; *Proc. ISMRM* 18 2010; 1768.

ISMRM 2013